


Improvement of Targeted Therapy by E. coli Phage-lysate Vaccination: Tumor Microenvironment Modulation and Magnetic Nanoparticle Delivery Enhancement in Tumor Tissue

 Ketevan Ghambashidze¹, Ramaz Chikhladze¹, Tamar Saladze¹,  Fridon Shubitidze²

DOI: [10.52340/GBMN.2023.01.01.09](https://doi.org/10.52340/GBMN.2023.01.01.09)

ABSTRACT

BACKGROUND.

The tumor microenvironment (TME) has an essential role in cancer development. TME reduces the drug and nanoparticle delivery in tumor tissue and minimizes the treatment outcomes. The new therapeutic strategies of TME reprogramming have shown great promise. One such strategy is TME modulation by the E. coli phage-lysate (EcPHL) vaccination with TME modification and enhancement of magnetic nanoparticles (mNP) uptake by tumor tissue.

OBJECTIVES

In the current study, we aimed to evaluate the effects of EcPHL vaccination on TME and mNP distribution in the tumor tissue.

METHODS

Experiments were carried out on 20-25 g BALB/c male mice. EcPHL intraperitoneal vaccinations (0,25 ml, 3x, with 3-day intervals) were initiated after 6 days of the Ehrlich ascites carcinoma (EAC) cells subcutaneous inoculation and intratumoral administration of mNP (5 mg/cm³) - on the 4th day after the last administration of EcPHL. Tumor volume was measured using a Vernier caliper. Tumor tissue samples, and the spread of mNPs in tumor tissue were estimated using microscope Leica DM6B, Motic Easy Scan Pro scanner (Ultrahigh NA APO 20X [NA 0,75], resolution 40X:0,25 mm/pixel).

RESULTS

The mean tumor volume (MTV) was significantly reduced in EcPHL-vaccinated mice. The morphological investigation has shown an increased number of immunocompetent cells, basically macrophages, around the atypical cells in the tumor stroma, infiltrating the inflammatory regions and necrotic areas in the center of the tumor tissue. The inflammatory infiltrations with macrophages were prevalent in the necrotic areas. After mNP injection, the pigment was spread at a distance from the injection site as concentrated masses in extracellular regions of tumor tissue. Areas of inflammatory infiltration and concentration of iron-containing cells were significantly higher in the EcPHL-vaccinated mice compared to unvaccinated, and iron-containing macrophages were detected at a much greater distance from the injection site.

CONCLUSIONS

EcPHL stimulates anticancer responses, inhibits tumor growth, and enhance the distribution of mNP in tumor tissue.

KEYWORDS

Cancer; E. coli phage-lysate (EcPHL); magnetic/iron nanoparticles (mNP); Tumor microenvironment (TME).

BACKGROUND

Despite the significant achievements in molecular biology and the newest treatment modalities, cancer remains the biggest challenge to the modern healthcare system.^{1,2}

The tumor microenvironment (TME), which plays a crucial role in the development and progression of cancer, consists of stroma, endothelial cells, pericytes, fibroblasts, smooth muscle, and immune cells; and is characterized by hypoxia, acidosis, and high interstitial fluid pressure.^{3,4}

TME is a major barrier and potential target for tumor-targeted treatment and the delivery of nanoparticles (NPs) in the tumor tissue. In addition to resistance to the extravasation and distribution of NPs, TME attenuates the treatment outcomes.⁵ TME also contains tumor-associated

macrophages (TAM, a type of immune cell), that are produced from circulating monocytes and bind the tumor site to cancer and stromal cells. TAMs, in general, are associated with promoting tumor growth and progression by the secretion of growth factors and cytokines that support neoangiogenesis, inhibition of the immune response, and promotion of tumor invasion and metastasis. The TAMs also play a crucial role in the remodeling of the extracellular matrix and tissue repair. However, TAMs also exhibit anti-tumor functions, such as phagocytosis of cancer cells and anti-tumor immune response due to the antigen presentation to the T-cells. Thus, the new targeted treatment enhancing the antitumor immunity and inhibiting the protumor effects of TAMs would be ideal.



The new strategies of TME and TAM modulation are aimed to inhibit tumor growth and improve the delivery of drugs and NPs to the tumor tissue with minimal adverse effects. It is important to consider that modulation of tumor stroma may lead to enhanced tumor migration and metastasis. Therefore, these strategies should be carefully designed and cautiously evaluated. More attention should be focused on seeking combination strategies for modulating TME.⁶

There is promising evidence of the effectiveness of bacteria/bacteria-derived membrane particles in the modulation of TME/TAM and the controlled targeted drug delivery to cancer. They can overcome physical barriers, target and accumulate in tumor tissues and initiate antitumor immune responses. The studies have shown that the bacteria and bacteria-derived membrane particles can affect TME, TAM, macrophage M1, and M2 phenotypes and support the transport of anticancer agents into tumor tissues with the safety and efficacy of treatment, but decreased cytotoxic effects in normal cells.⁷

In our previous studies, we found that the *E. coli* phage-lysate (EcPHL) vaccination can reduce tumor growth by 80–90% in 65 % of tumor-bearing mice without apparent side effects.⁸⁻¹¹ In 13% of cases, neoplasms in an average volume of 250 mm³ underwent complete regression on the 65th–69th days of malignant growth. Increased numbers of Natural Killer (NK) cells (NK1.1+), T cells (CD3+/CD4+, CD3+/CD8+), IFN- γ , and IL-12 were seen in vaccinated mice with Ehrlich carcinoma by flow cytometry and ELIS analysis. Morphological examination revealed the prevalence of macrophages in tumor tissue.⁸⁻¹¹

Considering the abovementioned anti-cancer immunomodulatory effects of EcPHL we aimed to evaluate the consequences of the EcPHL vaccination on TME modification and mNP delivery in the tumor tissue.

METHODS

Study animals

8- to 10-week-old male BALB/c mice weighing 20-25 g were purchased from the vivarium of the Alexander Natishvili Institute of Morphology (Tbilisi, Georgia. <https://www.tsu.ge/en>). After being placed in a laboratory (8 per cage), the animals were given a 7-day interval for acclimatization before the experiment. During this period, they were fed a standard laboratory chow and given free access to water.

Disease modeling

The Ehrlich ascites carcinoma (EAC) cells were kindly provided by the Kavetsky Institute of Experimental Pathology, Oncology, and Radiobiology of the National Academy of Sciences of Ukraine, Department of Experimental Cell Systems, The Cell Line Bank (BCL) from

Human and Animal Tissues (<https://iepor.org.ua/www.onconet.kiev.ua>).

The EAC cells were propagated in our laboratory biweekly through intra-peritoneal injections of 5×10⁶ cells/mouse. Cells were counted by the hemocytometer.

Under brief ether anesthesia, each mouse was inoculated subcutaneously in the right flank with a fixed number of viable cancer cells (2×10⁶ cells/20 g body weight) freshly drawn from a donor mouse to induce the formation of a solid tumor. The viability of the EAC cells was 98% (by trypan blue exclusion assay).

Biopreparation

The anticancer immunomodulatory biopreparation - EcPHL (*E. coli* phage lysate, titer 2×10¹⁰, fr.8) was provided by the George Eliava Institute of Bacteriophage, Microbiology and Virology, Laboratory of Microbial Ecology (Tbilisi, Georgia, <http://eliava-institute.org/>).

Iron magnetic nanoparticles (mNPs)

mNPs were provided by the Thayer School of Engineering, Dartmouth College, Hanover, NH, 03755 USA (Kekalo et al 2013, 2014, Shubitidze et al 2025, 2022).

Immunomodulation and administration of mNP

EcPHL intraperitoneal vaccinations (0,25 ml, fr.8, 3 times, with 3-day intervals) were initiated after 6 days of EAC inoculation when the average size of tumors was 0,3 cm³. Intratumor administration of mNP (5 mg/cm³) was conducted on the 4th day after the last administration of EcPHL.

Study group formation

Cancer-bearing mice were randomly divided into 4 groups:

- Group I: control group, animals received no treatment;
- Group II: EcPHL-vaccinated animals;
- Group III: animals received Fe-containing magnetic nanoparticles (mNPs), and
- Group IV: EcPHL-vaccinated animals received mNPs.

The length and width of the tumors were measured individually using a Vernier caliper. Ellipsoidal tumor volume was routinely controlled and assessed every third day and calculated using the formula: $V = \text{length} \times \text{width}^2 \times 0.52$.

Histological evaluation

The samples (tumor tissue) were taken from sacrificed animals 3 and 12 hours after mNP administration for assessment of time-dependent mNP distribution in tumor tissue. Hematoxylin and Eosin (H and E) and Perl's Prussian blue stained tissue samples were evaluated histologically under a microscope Leica DM6B. MotiC Easy Scan Pro scanner (Ultrahigh NA APO 20X [NA 0,75]. Resolution 40X:0,25 mm/pixel) was used for tumor tissue samples (H&E

and Perl's-stained glass microscope slides) scanning and measurement of mNPs spread in tumor tissue.

Statistical analysis

IBM SPSS was used for analyzing data. Differences between tumor control and treated animals were determined by using the Independent-Samples T-test. The criterion for significance was set to $p < 0.05$.

RESULTS

We found that anti-tumor immunomodulation with EcPHL-vaccination had a significant inhibitory effect on tumor growth compared to the control group: on the 9th day of Ehrlich carcinoma growth, the mean tumor volume in treated animals was less by 55.8% ($p < 0.002$), on the 12th day – by 62% ($p < 0.001$), on the 15th day – by 47% ($p < 0.001$), and on the 16th day – by 46% ($p < 0.001$) (Tab.1).

TABLE 1. Mean tumor volume (cm³) in treated (Group II: EcPHL-vaccination) and untreated (Group I: control) mice

| Days of Ehrlich carcinoma growth | N | Treated M±SD | Untreated M±SD | P value |
|------------------------------------|---|--------------|----------------|---------|
| MTV (cm ³) on 6th day | 8 | 0.32±0.4 | 0.34±0.4 | 0.930 |
| MTV (cm ³) on 9th day | 8 | 0.87±0.5 | 1.97±0.6 | 0.002 |
| MTV (cm ³) on 12th day | 8 | 0.83±0.5 | 2.21±0.6 | 0.000 |
| MTV (cm ³) on 15th day | 8 | 1.91±0.7 | 3.63±0.8 | 0.000 |
| MTV (cm ³) on 16th day | 8 | 2.54±0.8 | 4.74±1.1 | 0.000 |

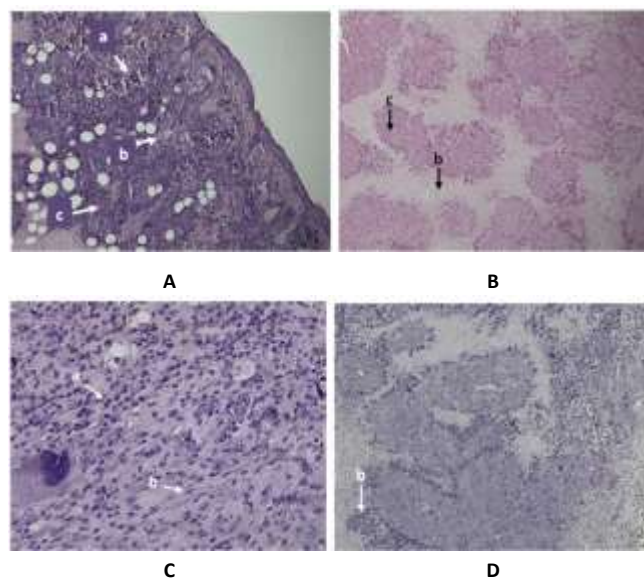
Abbreviations: MTV: mean tumor volume.

The well-developed atypical cells in derma, subcutaneous fat, and striated muscle tissue were detected by the histological evaluation of carcinoma-bearing control group mice samples (Fig.1). The tumor tissue was predominantly surrounded by connective tissue with polymorphonuclear leucocytes and neoplastic cells. The perinecrotic zones within the tumor were infiltrated by polymorphonuclear inflammatory cells. Certain areas of necrosis were coagulative and liquefactive as well.

Tumor tissue was presented by the parenchyma and well-vascularized stroma. Parenchyma predominantly consisted of atypical, anaplastic cells with abundant basophilic cytoplasm, characterized by well-expressed polymorphism, containing hyperchromic polymorph nucleus and clear nuclei with frequent mitotic figures, including atypical mitosis. Atypical cells were predominantly hyperchromic, small in size in the central areas of tumor tissue, and light and giant on the periphery (Fig.1).

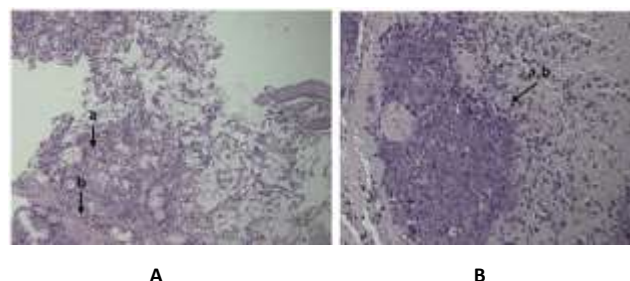
The increased number of immunocompetent cells (basically macrophages) around the tumor stroma infiltrating the central inflammatory regions and necrotic areas of tumor tissue were detected in EcPHL-vaccinated carcinoma-bearing mice of Group II (Fig.2).

FIGURE 1. Histological preparations of tumor tissue (Ehrlich carcinoma) of untreated mice (Group I)



Interpretations: Tissue samples A (H&E stain, x100) and B (H&E stain, x200) show the derma, subcutaneous fatty tissue and spread of atypical cells in striated muscle tissue (a). The tumor tissue is surrounded by connective tissue (b) with polymorphonuclear leucocytes and atypical/neoplastic cells. The tumor necrotic zones are surrounded by polymorph nuclear inflammatory cell infiltrates (c). Tissue samples C (H&E stain, x400) and D (H&E stain, x100) show predominantly hyperchromic and small atypical cells (a) in the central areas of tumor tissue, and light and giant atypical cells on the periphery (b).

FIGURE 2. Histological preparations of tumor tissue (Ehrlich carcinoma) of EcPHL-vaccinated mice (Group II)

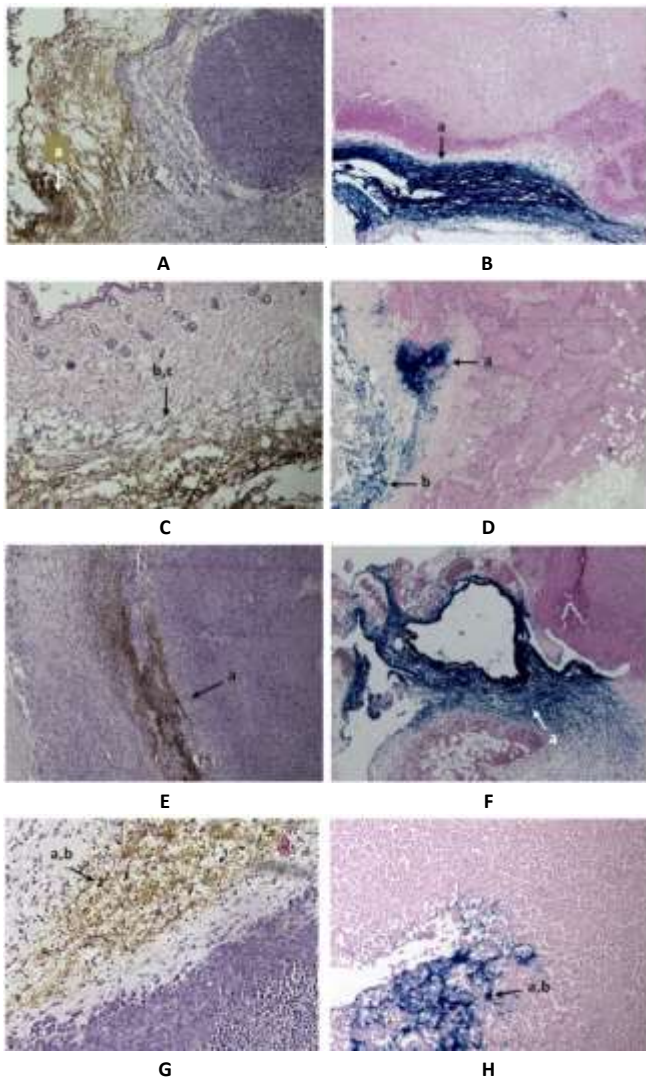


Interpretations: Tissue samples A (H&E stain, x100) and B (H&E stain, x200) show an increased number of macrophages (a) around the atypical cells in tumor stroma. Necrotic areas with inflammatory infiltrations and an abundant number of macrophages (b).

Tissue samples of the Group III carcinoma-bearing mice administered with mNP (samples taken after 3 hours of mNP intratumor injection) have shown accumulation of a considerable amount of exogenous pigment at the site of mNP injection (Fig.3A and Fig3B). The exogenous pigment was more in necrotic zones, connective and fat tissues supposedly due to the less density compared to tumor tissue and less resistance to mNP distribution (Fig.3C and Fig3D). The exogenous pigment was detected in extracellular areas in the form of concentrated masses and relatively rare in the form of large granules (Fig.3E and Fig.3F).

Tissue samples taken after 12 hours of mNP administration at the site of injection have shown accumulation of a considerable amount of exogenous pigment and iron-containing macrophages (Fig.3D and Fig.3H), which were relatively more compared to the samples taken after 3 hours of mNP administration.

FIGURE 3. Histological preparations of tumor tissue (Ehrlich carcinoma) of Group III mice after 3 and 12 hours mNP intratumor injection



Interpretations: Tissue samples A (H&E stain, x100) and B (Perl's Prussian blue stain, x100) show an accumulation of exogenous pigment (a) detected with Perl's reaction at the site of mNP injection. Tissue samples C (H&E stain, x100) and D (Perl's Prussian blue stain, x100) show the exogenous pigment more in necrotic zones (a), connective (b) and adipose tissues (c). Tissue samples E (H&E stain, x100) and F (Perl's Prussian blue stain, x100) show the exogenous pigment detected in extracellular areas in the forms of concentrated masses, and relatively rarely in the form of large granules (a). Tissue samples G (H&E stain, x100) and H (Perl's Prussian blue stain, x100) show the accumulation of a considerable amount of exogenous pigment (a) and iron-containing macrophages (b).

Tissue samples taken after 3 hours of mNP injection in the Group IV carcinoma-bearing and EcPHL-vaccinated mice have shown accumulation of a considerable amount of iron-containing exogenous pigment. The pigment was

accumulated intra- and extracellularly in the necrotic areas and subcutaneous fatty and connective tissues. The extracellular pigment was presented by a large number of concentrated masses.

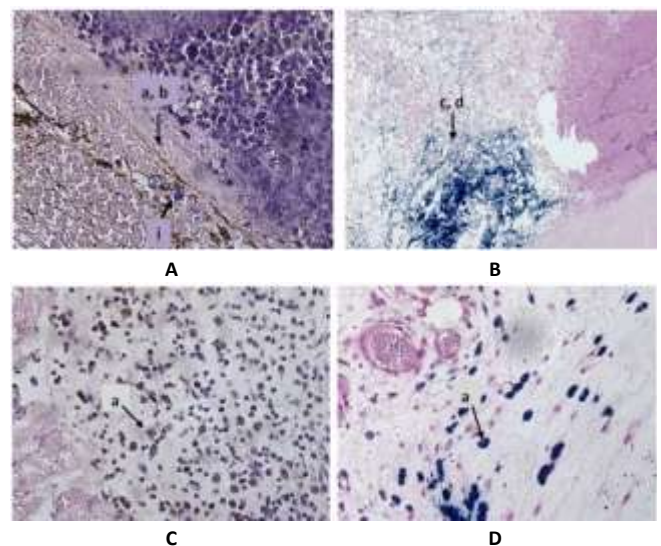
Macrophages were located near mNP accumulation areas (Fig.4A and Fig.4B). The cytoplasmic granules of intracellular iron-containing exogenous pigment were detected in inflammatory infiltrates, necrotic areas, and macrophages, mostly in connective and fatty tissues (Fig.4C and Fig.4D).

The number of inflammatory infiltration areas and quantity of iron-containing macrophages was significantly higher compared to Group III cancer-bearing mice (administered only with mNP). The intra-cytoplasmic pigment granules and distance and spread of iron-containing macrophages from the center of mNP injection were not significantly changed (Fig.4E and Fig.4F).

The iron-containing macrophages were detected at the site of extracellular pigment accumulation. The density and spread of iron-containing macrophages decrease gradually from the center to the periphery of pigment deposition (Fig.4G and Fig.4H).

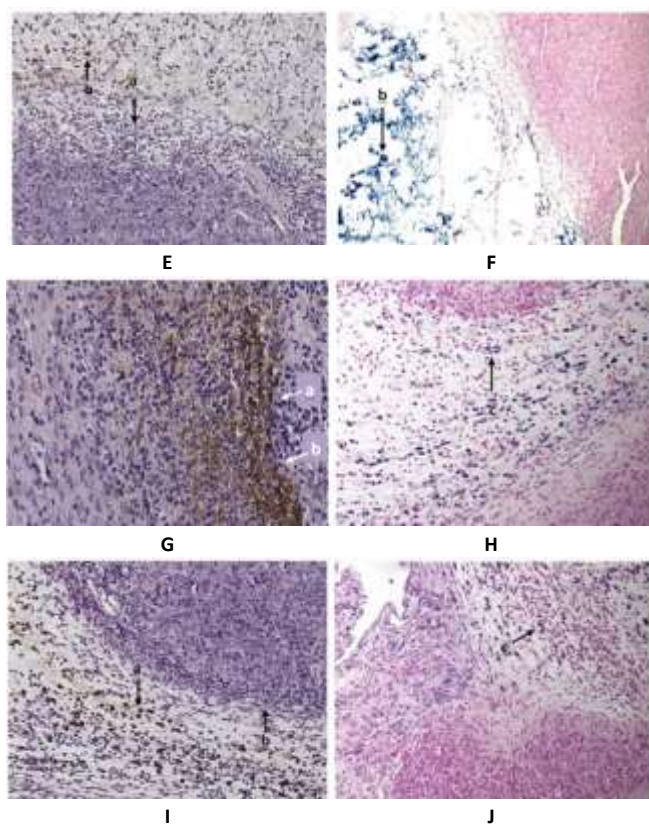
Tissue samples taken after 12 hours of mNP intratumoral injection demonstrated a large number of intra- and extracellular accumulations of concentrated masses of pigment in the necrotic areas, fatty and connective tissues. The iron-containing macrophages also were detected at more distance from mNP injection (Fig.4I and Fig.4J) compared to the samples taken after 3 hours.

FIGURE 4. Histological preparations of tumor tissue (Ehrlich carcinoma) of EcPHL-vaccinated Group IV mice after 3 hours mNP intratumor injection



Interpretations: Tissue samples A (H&E stain, x400) and B (Perl's Prussian blue stain, x100) show an accumulation of iron-containing exogenous pigment (a). The pigment accumulated in the necrotic areas, fatty and connective tissue (b) under the skin. Pigment is accumulated intra- and extra-cellularly (c). The extracellular pigment is presented by large amounts of concentrated masses (d). Macrophages are located near mNP accumulation (i). Tissue samples C (H&E stain, x400) and D (Perl's Prussian blue stain, x400) show intracellular iron-containing exogenous pigment in the form of cytoplasmic granules in inflammatory infiltrates (a), necrotic areas, and macrophages, mostly in connective and fatty tissues.

FIGURE 4. Histological preparations of tumor tissue (Ehrlich carcinoma) of EcPHL-vaccinated Group IV mice after 3 and 12 hours mNP intratumor injection (continued)



Interpretations: Tissue samples E (H&E stain, x200) and F (Perl's Prussian blue stain, x100) show lymphoplasmacytic inflammatory infiltration (a) and iron-containing macrophages (b). Tissue samples G (H&E stain, x200) and H (Perl's Prussian blue stain, x200) show extracellular pigment accumulation (a), iron-containing macrophages on the periphery (b). The density and spread of macrophages decrease gradually from the pigment deposition center to the periphery (c). Tissue samples I (H&E stain, x200) and J (Perl's Prussian blue stain, x200) show iron-containing exogenous pigment accumulation in the necrotic areas, fatty and connective tissues intra- and extracellularly (a). Large amounts of concentrated masses of pigment, inflammatory infiltration (b), and high-concentration macrophages (c).

DISCUSSION

Histological examination of tumor tissue samples has shown that in EcPHL-vaccinated mice the mNP were spread over more distance compared to the control. In the late hours after mNP administration, the pigment accumulated in the necrotic areas and fatty and connective tissues. Areas of inflammatory infiltration and concentration of iron-containing cells were more, and iron-containing macrophages were detected at a much more distance from mNP injection compared to non-vaccinated mice.

Facilitated distribution of mNPs in tumor tissue of EcPHL-vaccinated mice supposedly could be explained by anticancer immunomodulatory properties of EcPHL, altering the TME, shifting it toward the Th1 pathway, and reprogramming TAMs toward M1-like macrophages.

EcPHL-induced massive necrosis of tumor tissue activated mNP-containing macrophages to move in tumor

tissue due to their tropism to hypoxia, increasing therapeutic action against drug-resistant cells.¹²

Cancer cells are highly active in terms of their metabolic needs. Their survival and proliferation depend on the supply of important micro- and macronutrients. One of these crucial micronutrients is iron. Iron is essential for energy metabolism and DNA synthesis, which is one of the reasons why iron depletion causes cell cycle arrest.

Macrophages potentially deliver iron to cancer, supporting tumor promotion. M2 macrophages release iron into tumor tissues.^{13,14} M1 macrophages are characterized by ferritin high/ferroportin (Fpn) low phenotype, which tends to store iron, whereas M2 macrophages are characterized by elevated heme uptake and degradation, as well as ferritin low/Fpn high phenotype, which is believed to recirculate iron to the microenvironment.¹⁵

EcPHL vaccination affecting TME and producing shifting of M2 macrophages to M1 phenotype supposedly will interfere with adequate delivery of iron in tumor cells via reducing M2 macrophages. The increased concentration of M1 macrophages, additionally loaded with iron-containing mNPs will be easily delivered to the tumor cells.¹⁶⁻¹⁹

CONCLUSIONS

EcPHL has the potential for TME/TAM modification and enhancement of mNP delivery in and around tumor cells. It was demonstrated that EcPHL generates strong immunomodulation responses in and around TME and activates TAM.

As a result, the EcPHL:

- provides anticancer protection;
- significantly inhibits tumor growth;
- affects TME and facilitates the distribution of mNPs in tumor tissue.

In future studies, we plan to combine EcPHL immune modulator with the mNP-hyperthermia. We aim to activate mNP in the tumor using the external alternating electromagnetic fields and assess how mNP hyperthermia improves cancer treatment by shifting TAMs pro-tumor functions towards anti-tumor functions.

AUTHOR AFILIATION

¹Tbilisi State Medical University (TSMU), Tbilisi, Georgia;

²School of Engineering, Dartmouth College, Hanover, USA.

ACKNOWLEDGEMENTS

This work was supported by the School of Engineering, Dartmouth College, Hanover, USA. Authors are grateful to Dr. Marina Tediashvili (Head of the Laboratory of Microbial Ecology, Eliava Institute of Bacteriophages, Microbiology and Virology [EIBMV]), Dr. Eka Jaiani (Researcher at the Laboratory of Microbial Ecology, EIBMV) and Rusudan Aphrasidze (TSMU Ph.D. student, investigator at the Laboratory of Microbial Ecology, EIBMV) for construction of

phage lysate EcPHL and kindly providing for anticancer immunomodulation. We also thank Besarion Lasareishvili (the Agricultural University of Georgia, Laboratory of Cellular Immunology) and Prof. Nina Kulikova (the Agricultural University of Georgia, Head of the laboratory of cellular immunology) for their kind assistance in processing, counting, and propagation of cell culture.

REFERENCES

- Zhang, Z., Liu, X., Chen, D. et al. Radiotherapy combined with immunotherapy: the dawn of cancer treatment. *Sig Transduct Target Ther* 7, 258 (2022). <https://doi.org/10.1038/s41392-022-01102-y>.
- Nicole M. Anderson, M. Celeste Simon., "Tumor Microenvironment." *Curr Biol.* 2020 Aug 17;30(16):R921-R925. doi: 10.1016/j.cub.2020.06.081. *Curr Biol.* 2020 August 17; 30(16): R921–R925. Doi:10.1016/j.cub.2020.06.081.
- Toker A, Ohashi PS. Expression of costimulatory and inhibitory receptors in FoxP3(+) regulatory T cells within the tumor microenvironment: implications for combination immunotherapy approaches. *Adv Cancer Res.* 2019;144:193–261.
- Sakaguchi S, Mikami N, Wing JB, Tanaka A, Ichiyama K, Ohkura N. Regulatory T cells and human disease. *Annu Rev Immunol.* 2020; 38:541–66.
- Mingming Zhang, Shan Gao, Dongjuan Yang, Yan Fang, Xiaojie Lin, Xuechao Jin, Yuli Liu, Xiu Liu, Kexin Su, Kai Shi*Influencing factors and strategies of enhancing nanoparticles into tumors in vivo. *Acta Pharm Sin B.* 2021 Aug; 11(8): 2265–2285. Published online 2021 Mar 24. doi: 10.1016/j.apsb.2021.03.033. PMCID: PMC8424218, PMID: 34522587.
- Rilan Bai, Jiuwei Cui. Development of Immunotherapy Strategies Targeting Tumor Microenvironment Is Fiercely Ongoing. *Front Immunol.* 2022; 13: 890166. Published online 2022 Jun 27. doi: 10.3389/fimmu.2022.890166 PMCID: PMC9271663, PMID: 35833121.
- Zhenping Cao, Jinyao Liu. Bacteria and bacterial derivatives as drug carriers for cancer therapy. *Journal of Controlled Release.* 2020;(326): 396-407.
- Gambashidze K, Sepashvili A, Khorava P, Azaladze T, Jaiani E, Lasareishvili B, Tediashvili M. Gram-negative bacterial phage lysates in anticancer therapy. *JMed Microb Diagn.* 2017;6:2(Suppl)DOI: 10.4172/2161-0703-C1-006.
- Gambashidze K, Khorava P, Azaladze T, Kalendarishvili K, Jaiani E, Lasareishvili B, Azaladze A, Tediashvili M. Antitumor and adjuvant effects of phage lysates of *E. coli* in mice with Ehrlich carcinoma. *Exp Onco.* 2012;(34)2:1–5.
- Gambashidze K, Khorava P, Azaladze T, Azaladze A, Lasareishvili B, Jaiani E, Tediashvili M. Anti-tumor effects of phage lysates of *E. coli*. *Annals of Oncology.* 2012;(23),Suppl.2:17 /4th IMPAKT Breast Cancer Conference, Brussels, Belgium.
- Gambashidze K., Kalendarishvili K, Khorava P, Azaladze T, Lasareishvili B, Jaiani E, Tediashvili M. Efficacy of application of bacterial thermo- and phage lysates for suppression of malignant growth: a comparative analysis of the anti-cancer activity of *Ps.aeruginosa* and *E.coli* thermo-phage lysates (in Russian). *GeorgianMedical News.* 2012; (207),6:50-56. <https://geomednews.com/>.
- Ruixue Bai, Yunong Li, Lingyan Jian, Yuehui Yang, Lin Zhao, Minjie Wei . The hypoxia-driven crosstalk between tumor and tumor-associated macrophages: mechanisms and clinical treatment strategies. *Molecular Cancer.* 2022;(21),n:177. Published: 08 September 2022.
- Ying Chen Zhimin Fan Ye Yang Chunyan Gu. Iron metabolism and its contribution to cancer (Review). *International Journal of Oncology.* 2019,p.1143-1154.
- Duan X, He K, Li J, Cheng M, Song H, Liu J, et al. Tumor-associated macrophages deliver iron to tumor cells via Lcn2. *Int J Physiol Pathophysiol Pharmacol.* 2018, 10:105–14.
- Xiaoyue Duan, Kun He, Jing Li, Man Cheng, Hongjiao Song, Jinqiu Liu, Ping Liu. Tumor-associated macrophages deliver iron to tumor cells via Lcn2. *Int J Physiol Pathophysiol Pharmacol.* 2018; 10(2): 105–114.
- K. Kekalo and I. Baker, "Magnetic nanoparticles, composites, suspensions and collides with high specific absorption rate (SAR)". Patent 089464A1, December 2013.
- K. Kekalo, I. Baker, R. Meyers, and J. Shyong, "Magnetic nanoparticles with High Specific Absorption Rate at Low Alternating Magnetic Field," *Nano Life*, 2014.
- F. Shubitidze, K. Kekalo, R. Stigliano, and I. Baker "Magnetic nanoparticles with a high specific absorption rate of electromagnetic energy at low field strength for hyperthermia therapy", *Journal of Applied Physics* 117, (2015) Issue: 9; p. 094302.
- F. Shubitidze, K. Ghambashidze, and J. Hoopes, "A joint Phagelysate and mNP hyperthermia approach for cancer treatment", *European Society for Hyperthermic Oncology 34th Annual Meeting 14–17 September 2022, Gothenburg, Sweden.* https://www.esho2022.eu/fileadmin/congress/media/esho2022/druckelemente/ESHO22_Abstract_book.pdf.